

A MULTISCALE ABEL KERNEL AND APPLICATION IN VISCOELASTIC PROBLEM

WENLIN QIU*, TAO GUO†, YIQUN LI‡, XU GUO§, AND XIANGCHENG ZHENG¶

Abstract. We consider the variable-exponent Abel kernel and demonstrate its multiscale nature in modeling crossover dynamics from the initial quasi-exponential behavior to long-term power-law behavior. Then we apply this to an integro-differential equation modeling, e.g. mechanical vibration of viscoelastic materials with changing material properties. We apply the Crank-Nicolson method and the linear interpolation quadrature to design a temporal second-order scheme, and develop a framework of exponentially weighted energy argument in error estimate to account for the non-positivity and non-monotonicity of the multiscale kernel. Numerical experiments are carried out to substantiate the theoretical findings and the crossover dynamics of the model.

Key words. multiscale kernel, power-law, variable-exponent, integro-differential equation, error estimate

AMS subject classifications. 45K05, 65M12, 65M60

1. Introduction.

1.1. A multiscale kernel. We consider the following Abel kernel with the variable exponent $0 < \alpha(t) \leq 1$ [12, 35]

$$k(t) := \frac{t^{\alpha(t)-1}}{\Gamma(\alpha(t))} \quad (1.1)$$

where $\Gamma(\cdot)$ is the Euler's Gamma function. Compared with the commonly-used constant-exponent kernel ($\alpha(t) \equiv \alpha$ for some $0 < \alpha < 1$), which models the power-law phenomena in various applications [9, 14, 18], the variable-exponent kernel (1.1) could model more complex phenomena with multiple scales. A typical example is the normal-anomalous diffusion of the particles in worm-like micellar solutions observed in experiments in [17], which is a crossover dynamics with multiple diffusion scales in time such that a constant-exponent (i.e. single-scale) power-law kernel could not accommodate the transition between multiscale diffusion processes. Instead, it is shown in [40] that the variable-exponent kernel (1.1) with $\alpha(0) = 1$ provides a local modification of subdiffusion that could characterize the normal-anomalous diffusion process.

The success of describing the normal-anomalous diffusion process in [40] essentially relies on the multiscale feature of the variable-exponent kernel (1.1) with $\alpha(0) = 1$. To give a better understanding of its multiscale nature, we first select $\alpha(t) = 0.9 + 0.1e^{-0.1t}$ as an example, which satisfies the following asymptotics

$$\alpha(t) \sim \alpha(0) + \alpha'(0)t \text{ for } t \text{ small enough and } \alpha(t) \sim 0.9 \text{ for } t \text{ large enough.}$$

*School of Mathematics, Shandong University, Jinan 250100, China. (Email: wlqiu@sdu.edu.cn)

†School of Mathematics and Statistics, Hunan Normal University, Changsha, Hunan 410081, China. (Email: guotao6613@163.com)

‡School of Mathematics and Statistics, Wuhan University, Wuhan 430072, China. (Email: YiqunLi24@outlook.com)

§Geotechnical and Structural Engineering Center, Shandong University, Jinan 250061, China. (Email: guoxu@sdu.edu.cn)

¶Corresponding author. School of Mathematics, Shandong University, Jinan 250100, China. (Email: xzheng@sdu.edu.cn)

We employ these to compare the variable-exponent Abel kernel (1.1) with its local asymptotics at $t = 0$ and $t = \infty$

$$k_0(t) := \frac{t^{(\alpha(0)+\alpha'(0)t)-1}}{\Gamma(\alpha(0))} = e^{\alpha'(0)t \ln t}, \quad k_\infty(t) := \frac{t^{0.9-1}}{\Gamma(0.9)} = \frac{t^{-0.1}}{\Gamma(0.9)} \quad (1.2)$$

in Fig. 1.1(left), from which we observe that the variable-exponent kernel exhibits a crossover dynamics from the initial quasi-exponential behavior (modeled by k_0) to the long-term power-law decay (modeled by k_∞), indicating the multiscale feature of (1.1). By this means, the variable-exponent kernel k not only eliminates the initial rapid change and thus the initial singularity of the constant-exponent kernel k_∞ , but captures its long-time power-law behavior that k_0 does not exhibit. For these reasons, we call (1.1) the *multiscale kernel*.

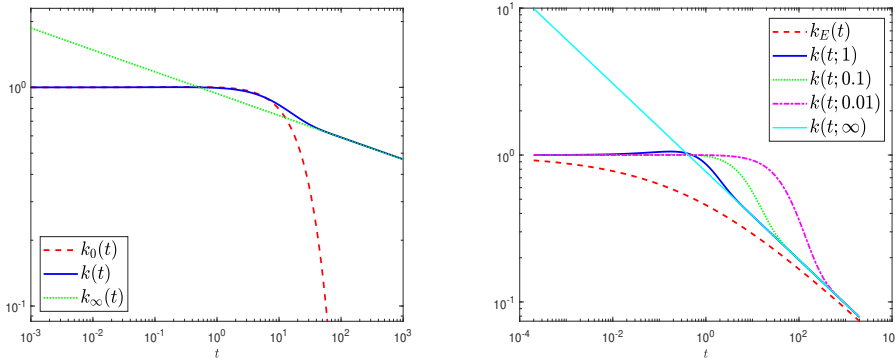


Fig. 1.1: Log-log plots of (left) $k(t)$ in (1.1) with $\alpha(t) = 0.9 + 0.1e^{-0.1t}$ and its asymptotics in (1.2) and (right) $k(t; a)$ with $\alpha(t; a) = 0.7 + 0.3e^{-at}$ for different a and the Mittag-Leffler kernel $k_E(t)$.

It is worth mentioning that similar multiscale features could also be realized by the well-known Mittag-Leffler kernel

$$k_E(t) := E_{\beta,1}(-t^\beta), \quad E_{\beta,1}(z) := \sum_{i=0}^{\infty} \frac{z^i}{\Gamma(\beta i + 1)}, \quad z \in \mathbb{R}$$

for some $0 < \beta < 1$. It is demonstrated in [3, Appendix B] and [27] that the Mittag-Leffler kernel behaves like a stretched exponential function, i.e. $e^{\frac{-t^\beta}{\Gamma(1+\beta)}}$, at short times with the stretching exponent β , and then exhibits a power-law decay like $\frac{t^{-\beta}}{\Gamma(1-\beta)}$ as t tends to infinity. Nevertheless, the proposed multiscale kernel (1.1) has the following advantages in comparison with the Mittag-Leffler kernel:

- As the Mittag-Leffler function is typically defined by an infinite series [19], it is difficult to evaluate the Mittag-Leffler kernel and the obtained value may not be accurate. In contrast, the multiscale kernel (1.1) could be simply evaluated with a very high accuracy.
- The Mittag-Leffler kernel gets close to the power law only if t tends to infinity, while the power law behaviors appear within finite times in most applications. Instead, the variable exponent provides a great flexibility in adjusting the properties of the kernel, which could account for more complicated scenarios.

To better illustrate the second statement, we present the curves of the Mittag-leffler kernel $k_E(t)$ with $\beta = 0.3$ and a parameterized multiscale kernel

$$k(t; a) = \frac{t^{\alpha(t; a)-1}}{\Gamma(\alpha(t; a))}, \quad \alpha(t; a) = 0.7 + 0.3e^{-at}$$

under different parameters a in Fig. 1.1(right). We observe that the Mittag-leffler kernel $k_E(t)$ approaches the power-law decay (modeled by $k(t; \infty) = \frac{t^{-0.3}}{\Gamma(0.7)}$) only for very large t , while the multiscale kernel could tend to the power-law decay at different times by adjusting the parameter a . Consequently, the above discussions demonstrate the flexibility and the novelty of the multiscale kernel (1.1) and motivate the application of this kernel in practical models.

1.2. Modeling issues. We apply the multiscale kernel (1.1) in the following parabolic integro-differential equation (PIDE), which attracts increasing attentions in viscoelastic material modeling [8, 13, 15]

$$\frac{\partial u}{\partial t}(\mathbf{x}, t) - \mu \Delta u(\mathbf{x}, t) - \zeta I^{(\alpha(t))} \Delta u(\mathbf{x}, t) = f(\mathbf{x}, t), \quad \mathbf{x} \in \Omega, \quad 0 < t \leq T \quad (1.3)$$

with the initial conditions

$$u(\mathbf{x}, 0) = u_0(\mathbf{x}), \quad \mathbf{x} \in \Omega \cup \partial\Omega \quad (1.4)$$

and boundary conditions

$$u(\mathbf{x}, t) = 0, \quad \mathbf{x} \in \partial\Omega, \quad 0 < t \leq T. \quad (1.5)$$

Here $\Omega \subset \mathbb{R}^d$ ($1 \leq d \leq 3$) is an open bounded smooth domain with boundary $\partial\Omega$, $T > 0$, the source term $f(\mathbf{x}, t)$ and the initial value $u_0(\mathbf{x})$ are given functions, $\mu > 0$ represents the viscosity coefficient, $\zeta > 0$, and the variable-exponent integral operator $I^{(\alpha(t))}$ is defined as follows [22, 30]

$$I^{(\alpha(t))} \varphi(t) = (k * \varphi)(t) := \int_0^t k(t-s) \varphi(s) ds. \quad (1.6)$$

In (1.3), the variable exponent determined by the characteristic fractal dimensions of the microstructures characterizes the structure changes of viscoelastic systems due to long-term cyclic loads, which in turn propagate to macro scales that eventually result in material failure [21, 25]. Furthermore, it is validated in [26] that the variable-exponent model may predict the compression deformation of amorphous glassy polymers with higher accuracy and fewer parameters, which motivates the application of the variable exponent in (1.3) to depict the changing physical properties of viscoelastic materials.

To demonstrate the impact of the multiscale kernel on solutions, we set $\Omega = (0, 1)$, $\mu = \zeta = 1$, $f \equiv 1$ and $u_0 = \sin(\pi x)$ in (1.3)-(1.5) and numerically compute $\partial_t u(0.5, t)$ over a short time period $[0, 0.1]$ under a multiscale kernel and a constant-exponent kernel, respectively, in Fig 1.2, which indicates that the condition $\alpha(0) = 1$ effectively eliminates the initial singularity of the solutions as shown in the case $\alpha(t) \equiv 0.2$. This phenomenon again indicates the advantage of the multiscale kernel and will be rigorously proved in Theorem 3.4.

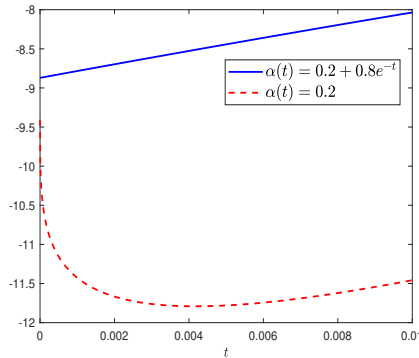


Fig. 1.2: Plots of $\partial_t u(0.5, t)$ under different $\alpha(t)$.

1.3. Novelty and contribution. For the case $\alpha(t) \equiv \bar{\alpha}$ for some $0 < \bar{\alpha} \leq 1$, there exist extensive mathematical analysis results for the PIDE (1.3) [10, 13, 15, 16, 39]. For numerical approximation, different numerical methods have been considered for PIDEs and their variants, such as finite element methods [4, 5, 28], discontinuous Galerkin methods [20, 29], convolution quadrature methods [36, 37], orthogonal spline collocation methods [31, 38], finite difference methods [33, 34] and so on. Nevertheless, rigorous mathematical and numerical analysis to model (1.3) is not available. In particular, due to the non-positive and non-monotonic nature of (1.1), many existing time discretization methods for the constant-exponent analogue of (1.6), such as convolution quadrature rule [23] and Laplace transform technique [24], may not be applicable. In a recent work [40], the resolvent estimates are adopted to analyze a multiscale diffusion model, which, after reformulation, takes a similar form as (1.3). Then a first-order-in-time scheme is accordingly developed and analyzed for the multiscale diffusion model in [40], which also applies for the viscoelastic model (1.3)-(1.5).

The current work considers a second-order-in-time scheme for the model (1.3)-(1.5), which improves the numerical method in [40]. To construct a second-order scheme, high-order solution regularity estimates are analyzed, and then we employ the Crank-Nicolson method and the linear interpolation quadrature to discretize temporal operators. To account for the non-positivity and non-monotonicity of (1.1), a framework of exponentially weighted energy argument is developed in numerical analysis, including modifying the difference quotient (cf. (4.2)), numerical scheme, and error equation, selecting a special test function (cf. (4.15)), etc. Numerical accuracy is rigorously proved and then verified by experiments. Furthermore, a crossover dynamics is observed when we model mechanical vibration by (1.3)-(1.5), which substantiates the multiscale feature of this viscoelastic model.

The rest of the paper is organized as follows. In Section 2 we present some preliminaries to be used subsequently. In Section 3, we derive the well-posedness and high-order regularity estimates of the solutions to (1.3)-(1.5). In Section 4, we construct a second-order numerical scheme and then prove its stability and error estimate. Numerical experiments are performed in the last section to substantiate the theoretical findings.

2. Preliminaries.

2.1. Notations. Let $L^p(\Omega)$ with $1 \leq p \leq \infty$ be the Banach space of p th power Lebesgue integrable functions on Ω . Given a positive integer m , let $W^{m,p}(\Omega)$ be the Sobolev space of L^p functions with the m th weakly derivatives in $L^p(\Omega)$. Let $H^m(\Omega) := W^{m,2}(\Omega)$ and $H_0^m(\Omega)$ be its subspace with the zero boundary condition reach order $m - 1$. For a non-integer $s \geq 0$, $H^s(\Omega)$ is defined through interpolation, see [1]. Let $\{\lambda_i, \phi_i\}_{i=1}^\infty$ be eigenpairs of the problem $-\Delta\phi_i = \lambda_i\phi_i$ on Ω with zero boundary conditions. Then, we introduce the Sobolev space $\check{H}^s(\Omega)$ with $s \geq 0$ by

$$\check{H}^s(\Omega) := \left\{ v \in L^2(\Omega) : \|v\|_{\check{H}^s(\Omega)}^2 := \sum_{i=1}^\infty \lambda_i^s (v, \phi_i)^2 < \infty \right\},$$

which is a subspace of $H^s(\Omega)$ and satisfies $\check{H}^0(\Omega) = L^2(\Omega)$ and $\check{H}^2(\Omega) = H^2(\Omega) \cap H_0^1(\Omega)$ [19]. For a Banach space \mathcal{X} , let $W^{m,p}(0, T; \mathcal{X})$ be the space of functions in $W^{m,p}(0, T)$ with respect to $\|\cdot\|_{\mathcal{X}}$. All spaces in this paper are equipped with standard norms [1, 11].

Throughout this paper, we use Q to denote a generic constant which may be different in different situations. We set $\|\cdot\| := \|\cdot\|_{L^2(\Omega)}$ and $L^p(\mathcal{X})$ for $L^p(0, T; \mathcal{X})$ for brevity, and remove the notation Ω in the spaces and norms if there is no confusion. For instance, $\|\cdot\|_{L^p(L^2)}$ implies $\|\cdot\|_{L^p(0, T; L^2(\Omega))}$. Furthermore, we make the **Assumption A**:

- (i) $0 < \alpha_* \leq \alpha(t) \leq 1$, $\alpha(0) = 1$ and $|\alpha'(t)|, |\alpha''(t)| \leq Q$ on $[0, T]$.
- (ii) $f \in L^p(L^2)$ for $1 < p < \infty$ and $\Delta u_0 \in L^2$.

2.2. Solution representation. Let Γ_θ be a contour in the complex plane for $\theta \in (\pi/2, \pi)$ and $\delta > 0$, defined as follows

$$\Gamma_\theta := \{z \in \mathbb{C} : |\arg(z)| = \theta, |z| \geq \delta\} \cup \{z \in \mathbb{C} : |\arg(z)| \leq \theta, |z| = \delta\}.$$

For $0 < \hat{\mu} \leq 1$ and $Q = Q(\theta, \hat{\mu})$, the following inequalities hold [2, 23]

$$\int_{\Gamma_\theta} |z|^{\hat{\mu}-1} |e^{tz}| |dz| \leq Qt^{-\hat{\mu}}, \quad \left\| \int_{\Gamma_\theta} z^{\hat{\mu}} (z - \mu\Delta)^{-1} e^{tz} dz \right\|_{L^2 \rightarrow L^2} \leq \frac{Q}{t^{\hat{\mu}}}, \quad t \in (0, T]. \quad (2.1)$$

For any $q \in L_{loc}^1(0, \infty)$ such that $|q(t)| \leq Qe^{\bar{\sigma}t}$ for large t and for some positive constants Q and $\bar{\sigma}$, we denote the Laplace transform \mathcal{L} of $q(t)$ as

$$\mathcal{L}q(z) := \int_0^\infty \tilde{q}(t) e^{-tz} dt, \quad \Re(z) > \bar{\sigma},$$

where \Re denotes the real part of a complex number. Following [23], if $\mathcal{L}q$ is analytic in a sector $\arg(z) < \bar{\chi}$ for some $\bar{\chi} \in (\pi/2, \pi)$ and satisfies that $|(\mathcal{L}q)(z)| \leq Q|z|^{-\hat{\mu}}$ for some $Q, \hat{\mu} > 0$, we denote the corresponding inverse transform \mathcal{L}^{-1} of $\mathcal{L}q$ in terms of the contour Γ_θ with $\theta < \bar{\chi}$ as

$$\mathcal{L}^{-1}(\mathcal{L}q(z)) := \frac{1}{2\pi i} \int_{\Gamma_\theta} e^{tz} \mathcal{L}q(z) dz = q(t). \quad (2.2)$$

Let $E(t) := e^{\mu t \Delta}$ be the semigroup of operators defined by $\partial_t E(t)g - \mu \Delta E(t)g = 0$ with $E(t)g = 0$ for $\mathbf{x} \in \partial\Omega$ and $E(t)g|_{t=0} = g$ for $\mathbf{x} \in \Omega$. The solution u of the following initial-boundary-value problem

$$\begin{aligned} \partial_t u(\mathbf{x}, t) - \mu \Delta u(\mathbf{x}, t) &= f(\mathbf{x}, t), \quad (\mathbf{x}, t) \in \Omega \times (0, T], \\ u(\mathbf{x}, t) &= 0, \quad (\mathbf{x}, t) \in \partial\Omega \times (0, T], \quad u(\mathbf{x}, 0) = 0, \quad \mathbf{x} \in \Omega \end{aligned} \quad (2.3)$$

can be expressed in terms of the $E(t)$ via the Duhamel's principle

$$u(\mathbf{x}, t) = \int_0^t E(t - \theta) f(\mathbf{x}, \theta) d\theta, \quad (2.4)$$

where $E(t)$ could be expressed for $\psi \in L^2(\Omega)$

$$E(t)\psi(\mathbf{x}) = \sum_{i=1}^{\infty} e^{-\mu\lambda_i t} (\psi, \phi_i) \phi_i(\mathbf{x}) = \frac{1}{2\pi i} \int_{\Gamma_\theta} e^{zt} (z - \mu\Delta)^{-1} \psi(\mathbf{x}) dz. \quad (2.5)$$

For $s \geq r \geq -1$ and any $t > 0$, the following estimates hold [2, 19, 23]

$$\|E(t)\|_{L^2 \rightarrow L^2} \leq Q, \quad \|E(t)\psi\|_{\dot{H}^s} \leq Qt^{-(s-r)/2} \|\psi\|_{\dot{H}^r}, \quad \psi \in \dot{H}^r. \quad (2.6)$$

Under the **Assumption A**, we invoke l'Hospital's rule to obtain

$$\begin{aligned} \lim_{t \rightarrow 0^+} [\alpha(t) - 1] \ln(t) &= \lim_{t \rightarrow 0^+} \frac{\alpha(t) - 1}{(1/\ln(t))} = \lim_{t \rightarrow 0^+} t \ln^2(t) \alpha'(t) = 0, \\ \lim_{y \rightarrow s^+} \frac{(y-s)^{\alpha(y-s)-1}}{\Gamma(\alpha(y-s))} &= \lim_{y \rightarrow s^+} \frac{e^{[\alpha(y-s)-1] \ln(y-s)}}{\Gamma(\alpha(y-s))} = 1, \end{aligned}$$

and we thus introduce the following estimates that are often used in subsequent analysis [32]

$$\begin{aligned} (t-s)^{\alpha(t-s)-1} &= e^{[\alpha(t-s)-1] \ln(t-s)} \leq Q, \\ \int_0^T e^{-\gamma t} t^{\hat{\mu}-1} dt &\leq \gamma^{-\hat{\mu}} \int_0^\infty e^{-s} s^{\hat{\mu}-1} ds = \gamma^{-\hat{\mu}} \Gamma(\hat{\mu}), \quad 0 < \hat{\mu} < 1. \end{aligned} \quad (2.7)$$

3. Mathematical analysis. We shall perform mathematical analysis for (1.3)-(1.5). In general, the well-posedness could be proved following the methods in [40] such that we only give the results without proof. For higher solution regularity that [40] does not cover, we give a detailed proof in order to support the construction of high-order numerical scheme.

We first refer the following properties of k from [40, Lemma 3.2].

LEMMA 3.1. *Assume **Assumption A** holds. Then, there exists a positive constant Q such that*

$$|k(t)| \leq Q, \quad |k'(t)| \leq Q(1 + |\ln(t)|), \quad |k''(t)| \leq Qt^{-1}. \quad (3.1)$$

Then the well-posedness could be proved following [40, Theorem 3.1].

THEOREM 3.2. *Under **Assumption A**, the problem (1.3) has a unique solution $u \in W^{1,p}(L^2) \cap L^p(\dot{H}^2)$ for $1 < p < \infty$, and*

$$\|u\|_{W^{1,p}(L^2)} + \|u\|_{L^p(\dot{H}^2)} \leq Q(\|f\|_{L^p(L^2)} + \|\Delta u_0\|_{L^2}).$$

To prove the high-order regularity estimates of the solutions, we move the convolution term in (1.3) to its right-hand side and then use the solution representation (2.4) to get

$$u = \left[E(t)u_0 + \int_0^t E(t-\theta) f(\mathbf{x}, \theta) d\theta \right] + \int_0^t E(t-\theta) \zeta(k * \Delta u)(\mathbf{x}, \theta) d\theta := \Xi_1 + \Xi_2. \quad (3.2)$$

Then we follow the proofs of [40, Lemma 4.1 and Theorem 4.2] to prove Lemma 3.3 and Theorem 3.4, respectively. Due to the similarity, we omit the proofs for simplicity.

LEMMA 3.3. *Assume **Assumption A** holds and $\alpha \in W^{3,\infty}(0, T)$. For $0 < t \leq T$ and $0 \leq \varepsilon \ll 1$, there exists a positive constant $Q = Q(\varepsilon, \|\alpha\|_{W^{3,\infty}}, T)$ such that*

$$|\partial_t I^{(1-\varepsilon)} \partial_t (\zeta(k * \Delta v))| \leq Q \int_0^t \frac{|\partial_s \Delta v(\mathbf{x}, s)| ds}{(t-s)^\varepsilon} + \frac{Q|\Delta v_0|}{t^\varepsilon}, \quad v = u \text{ or } \Delta u. \quad (3.3)$$

THEOREM 3.4. *Suppose **Assumption A** holds and $\alpha \in W^{3,\infty}(0, T)$, $u_0 \in \dot{H}^4$ and $f \in W^{1,p}(L^2) \cap L^p(\dot{H}^{2+\sigma})$ for $0 < \sigma \ll 1$ and $1 \leq p \leq \infty$, then the solution of (1.3) satisfies*

$$\begin{aligned} & \|u\|_{W^{2,p}(L^2)} + \|u\|_{L^\infty(\dot{H}^2)} + \|u\|_{W^{1,p}(\dot{H}^2)} \\ & \leq Q(\|f\|_{W^{1,p}(L^2)} + \|f\|_{L^p(\dot{H}^{2+\sigma})} + \|u_0\|_{\dot{H}^4}). \end{aligned} \quad (3.4)$$

Now we give a detailed proof for higher regularity of the solutions that [40] does not cover.

THEOREM 3.5. *Suppose **Assumption A** holds and $\alpha \in W^{4,\infty}(0, T)$, $u_0 \in \dot{H}^6$ and $f \in W^{2,p}(L^2) \cap W^{1,p}(\dot{H}^2) \cap L^p(\dot{H}^{4+\sigma})$ for $0 < \sigma \ll 1$ and $1 \leq p < \infty$. Then the following estimates hold*

$$\|u\|_{W^{2,p}(\dot{H}^2)} \leq Q \left(\|f\|_{W^{1,p}(\dot{H}^2)} + \|f\|_{L^p(\dot{H}^{4+\sigma})} + \|u_0\|_{\dot{H}^6} \right), \quad (3.5)$$

$$\begin{aligned} \|u\|_{W^{3,p}(L^2)} & \leq Q \left(\|u_0\|_{\dot{H}^6} + \|f\|_{W^{1,p}(\dot{H}^2)} + \|f\|_{L^p(\dot{H}^{4+\sigma})} + \|f\|_{W^{2,p}(L^2)} \right) \\ & \quad + Qt^{-\varepsilon} \|\Delta u_0\|_{L^2}, \quad 0 < \varepsilon \ll 1. \end{aligned} \quad (3.6)$$

Proof. We first prove (3.5). Note that $\partial_t^2 \Delta u = \partial_t^2 \Delta \Xi_1 + \partial_t^2 \Delta \Xi_2$. By (2.5), we have $E''(t) \Delta u_0 = \mu^2 \Delta E(t) \Delta^2 u_0 = \mu^2 E(t) \Delta^3 u_0$ by $u_0 \in \dot{H}^6$, and we directly compute $\partial_t^2 \Delta \Xi_1$ in (3.2) to get

$$\begin{aligned} \partial_t^2 \Delta \Xi_1 & = \mu^2 E(t) \Delta^3 u_0 + \partial_t \Delta f + \mu \Delta^2 f + \mu^2 \int_0^t \sum_{i=1}^{\infty} \lambda_i^2 e^{-\mu \lambda_i (t-s)} (\Delta f, \phi_i) \phi_i ds \\ & = \mu^2 E(t) \Delta^3 u_0 + \partial_t \Delta f + \mu \Delta^2 f + \mu \int_0^t E'(t-s) \Delta^2 f(\mathbf{x}, s) ds. \end{aligned} \quad (3.7)$$

We first use (2.6) to obtain

$$\begin{aligned} \int_0^t \|E'(t-s) \Delta^2 f(\cdot, s)\|_{L^2(\Omega)} ds & \leq Q \int_0^t \|E(t-s) \Delta^2 f(\cdot, s)\|_{\dot{H}^2} ds \\ & \leq Q \int_0^t (t-s)^{-\frac{2-\sigma}{2}} \|\Delta^2 f(\cdot, s)\|_{\dot{H}^\sigma} ds \end{aligned}$$

for $0 < \sigma \ll 1$, which together with (3.7) gives

$$\begin{aligned} \|\partial_t^2 \Delta \Xi_1\|_{L^2(\Omega)} & \leq Q(\|E(t)\|_{L^2 \rightarrow L^2} \|\Delta^3 u_0\|_{L^2} + \|\partial_t \Delta f\|_{L^2} + \|\Delta^2 f\|_{L^2}) \\ & \quad + Q \int_0^t \|E'(t-s) \Delta^2 f(\cdot, s)\|_{L^2} ds \\ & \leq Q(\|\Delta^3 u_0\|_{L^2} + \|\partial_t \Delta f\|_{L^2} + \|\Delta^2 f\|_{L^2}) \\ & \quad + Q \int_0^t (t-s)^{-\frac{2-\sigma}{2}} \|\Delta^2 f(\cdot, s)\|_{\dot{H}^\sigma} ds. \end{aligned} \quad (3.8)$$

We take $\|\cdot\|_{L^p(0,T)}$ norm on both sides of (3.8) and apply Young's inequality to obtain

$$\begin{aligned} \|\partial_t^2 \Delta \Xi_1\|_{L^p(L^2)} &\leq Q(\|\Delta^3 u_0\|_{L^2} + \|f\|_{W^{1,p}(\check{H}^2)} + \|\Delta^2 f\|_{L^p(L^2)}) \\ &\quad + Q\|t^{-\frac{2-\sigma}{2}} * \|\Delta^2 f\|_{\check{H}^\sigma}\|_{L^p(0,T)} \\ &\leq Q(\|\Delta^3 u_0\|_{L^2} + \|f\|_{W^{1,p}(\check{H}^2)} + \|f\|_{L^p(\check{H}^{4+\sigma})}). \end{aligned} \quad (3.9)$$

Next, we shall discuss the analysis of $\partial_t^2 \Delta \Xi_2$. We utilize the commutativity of the convolution operator to deduce that

$$\begin{aligned} \partial_t \int_0^t E'(t-s) (\zeta(k * \Delta u)(\mathbf{x}, s)) ds &= \partial_t \int_0^t E'(s) (\zeta(k * \Delta u)(\mathbf{x}, y))|_{y=t-s} ds \\ &= \int_0^t E'(s) \partial_t (\zeta(k * \Delta u)(\mathbf{x}, y))|_{y=t-s} ds = - \int_0^t E'(t-s) \partial_s (\zeta(k * \Delta u)(\mathbf{x}, s)) ds. \end{aligned}$$

Differentiate Ξ_2 in (3.2) twice with respect to t and apply the above resulting equation to obtain

$$\begin{aligned} \partial_t \Delta \Xi_2 &= \int_0^t E'(t-s) (\zeta(k * \Delta^2 u)(\mathbf{x}, s)) ds + \zeta(k * \Delta^2 u)(\mathbf{x}, t), \\ \partial_t^2 \Delta \Xi_2 &= - \int_0^t E'(t-s) \partial_s (\zeta(k * \Delta^2 u)(\mathbf{x}, s)) ds + \partial_t (\zeta(k * \Delta^2 u)(\mathbf{x}, t)). \end{aligned} \quad (3.10)$$

Now, we utilize the following estimate

$$|\partial_t (\zeta(k * \Delta^2 u))| \leq Q \int_0^t |\partial_\theta \Delta^2 u| d\theta + Q |\Delta^2 u_0| \quad (3.11)$$

to directly bound the second term on the right-hand side of (3.10) and follow (2.2) and the similar procedures in [40, (3.14)-(3.15)] to reformulate

$$\begin{aligned} &\int_0^t E'(t-s) \partial_s (\zeta(k * \Delta^2 u)(\mathbf{x}, s)) ds \\ &= \int_0^t \left[\frac{1}{2\pi i} \int_{\Gamma_\theta} z^{1-\varepsilon} (z - \mu\Delta)^{-1} e^{z(t-s)} dz \right] (\partial_s I^{(1-\varepsilon)} \partial_s (\zeta(k * \Delta^2 u)(\mathbf{x}, s))) ds. \end{aligned}$$

We invoke (2.1) and (3.3) to bound the integral in the square brackets and the first term on the right-hand side in (3.10), respectively, to obtain

$$\begin{aligned} &\left\| \int_0^t E'(t-s) \partial_s (\zeta(k * \Delta^2 u)(\mathbf{x}, s)) ds \right\|_{L^2} \\ &\leq Q \int_0^t \frac{\|\partial_s I^{(1-\varepsilon)} \partial_s (\zeta(k * \Delta^2 u)(\mathbf{x}, s))\|_{L^2} ds}{(t-s)^{1-\varepsilon}} \\ &\leq Q \int_0^t \frac{1}{(t-s)^{1-\varepsilon}} \left(\int_0^s \frac{\|\partial_\theta \Delta^2 u(\cdot, \theta)\|_{L^2}}{(s-\theta)^\varepsilon} d\theta + \|\Delta^2 u_0\| s^{-\varepsilon} \right) ds \\ &\leq Q \int_0^t \|\partial_\theta \Delta^2 u(\cdot, \theta)\|_{L^2} d\theta + Q \|\Delta^2 u_0\|, \end{aligned} \quad (3.12)$$

where we swapped the order of the integral in the last inequality.

Fixing $1 \leq p < \infty$, and then we can select $0 < \varepsilon \ll 1$ to satisfy $0 < \varepsilon p < 1$. By multiplying $\partial_t^2 \Delta \Xi_2$ in (3.10) by $e^{-\gamma t}$ and taking the $\|\cdot\|_{L^p(0,T)}$ norm on both sides of the resulting equation, we then incorporate (2.7), (3.11), (3.12), and Young's convolution inequality to arrive at

$$\begin{aligned} \|e^{-\gamma t} \partial_t^2 \Delta \Xi_2\|_{L^p(L^2)} &\leq Q \|(e^{-\gamma t}) * (e^{-\gamma t} \|\partial_t \Delta^2 u(\cdot, t)\|)\|_{L^p(0,T)} + Q \|\Delta^2 u_0\| \\ &\leq Q \gamma^{-1} \|e^{-\gamma t} \partial_t \Delta^2 u\|_{L^p(L^2)} + Q \|\Delta^2 u_0\|. \end{aligned} \quad (3.13)$$

We differentiate (3.2) twice in time, apply the $\|\cdot\|_{L^p(0,T)}$ norm on both sides of the resulting equation, then multiply it by $e^{-\gamma t}$, and invoking (3.9) and (3.13) to get

$$\begin{aligned} \|e^{-\gamma t} \partial_t^2 \Delta u\|_{L^p(L^2)} &\leq \|e^{-\gamma t} \partial_t^2 \Delta \Xi_1\|_{L^p(L^2)} + \|e^{-\gamma t} \partial_t^2 \Delta \Xi_2\|_{L^p(L^2)} \\ &\leq Q (\|f\|_{W^{1,p}(\check{H}^2)} + \|f\|_{L^p(\check{H}^{4+\sigma})} + \|\Delta^2 u_0\| + \|\Delta^3 u_0\|) \\ &\quad + Q \gamma^{-1} \|e^{-\gamma t} \partial_t \Delta^2 u\|_{L^p(L^2)}. \end{aligned} \quad (3.14)$$

We then differentiate (3.2) with respect to t , apply the $\|\cdot\|_{L^p(0,T)}$ norm on both sides of the resulting equation multiplied by $e^{-\gamma t}$, and combine the estimates (3.11), (3.14) with Young's convolution inequality to bound

$$\begin{aligned} \|e^{-\gamma t} \partial_t \Delta^2 u\|_{L^p(L^2)} &\leq Q \|e^{-\gamma t} (\partial_t^2 \Delta u - \partial_t \Delta f - \partial_t (\zeta(k * \Delta^2 u)))\|_{L^p(L^2)} \\ &\leq Q (\|f\|_{W^{1,p}(\check{H}^2)} + \|f\|_{L^p(\check{H}^{4+\sigma})} + \|u_0\|_{\check{H}^6}) \\ &\quad + Q \gamma^{-1} \|e^{-\gamma t} \partial_t \Delta^2 u\|_{L^p(L^2)}. \end{aligned}$$

Here we set γ large enough to eliminate the last term on the right-hand side of the above equation to obtain

$$\|e^{-\gamma t} \partial_t \Delta^2 u\|_{L^p(L^2)} \leq Q (\|f\|_{W^{1,p}(\check{H}^2)} + \|f\|_{L^p(\check{H}^{4+\sigma})} + \|u_0\|_{\check{H}^6}),$$

which combined with (3.14) leads to

$$\|\partial_t^2 u\|_{L^p(\check{H}^2)} \leq Q \left(\|u_0\|_{\check{H}^6} + \|f\|_{W^{1,p}(\check{H}^2)} + \|f\|_{L^p(\check{H}^{4+\sigma})} \right). \quad (3.15)$$

This yields (3.5).

To prove (3.6), we shall bound $\|\partial_t^3 u\|_{L^p(L^2)}$. We apply the initial condition $\partial_t u(\mathbf{x}, 0) = \mu \Delta u_0 + f(\mathbf{x}, 0)$ from (1.3), the following relation

$$\partial_t^2 \int_0^t k(s) \Delta u(\mathbf{x}, t-s) ds = k'(t) \Delta u_0 + k(t) \Delta \partial_t u(\mathbf{x}, 0) + \int_0^t k(s) \partial_t^2 \Delta u(\mathbf{x}, t-s) ds,$$

and (1.3) to obtain

$$\begin{aligned} \partial_t^3 u &= \mu \partial_t^2 \Delta u + \zeta \partial_t^2 \int_0^t k(s) \Delta u(\mathbf{x}, t-s) ds + \partial_t^2 f(t) \\ &= \mu \partial_t^2 \Delta u + \partial_t^2 f(t) + \zeta k'(t) \Delta u_0 + \zeta k(t) [\mu \Delta^2 u_0 + \Delta f(\mathbf{x}, 0)] \\ &\quad + \zeta \int_0^t k(s) \partial_t^2 \Delta u(\mathbf{x}, t-s) ds. \end{aligned}$$

We combine (3.5) and (3.1) in Lemma 3.1, i.e., $|k'(t)| \leq Q(1 + |\ln(t)|) \leq Qt^{-\varepsilon}$, and the Sobolev embedding $W^{1,p}(0, T) \hookrightarrow L^\infty(0, T)$ [1] to obtain

$$\begin{aligned}
\|\partial_t^3 u\|_{L^p(L^2)} &\leq Q(\|\partial_t^2 \Delta u\|_{L^p(L^2)} + \|\partial_t^2 f(t)\|_{L^p(L^2)} + |k'(t)| \|\Delta u_0\|_{L^2}) \\
&\quad + Q|k(t)| [\|\Delta^2 u_0\|_{L^2} + \|\Delta f(\cdot, 0)\|_{L^2}] \\
&\quad + Q \int_0^t |k(s)| \|\partial_t^2 \Delta u(\cdot, t-s)\|_{L^p(L^2)} ds \\
&\leq Q(\|u_0\|_{\dot{H}^6} + \|f\|_{W^{1,p}(\dot{H}^2)} + \|f\|_{L^p(\dot{H}^{4+\sigma})} + \|f\|_{W^{2,p}(L^2)} + \|\Delta f(\cdot, 0)\|_{L^2}) \\
&\quad + Qt^{-\varepsilon} \|\Delta u_0\|_{L^2} \\
&\leq Q(\|u_0\|_{\dot{H}^6} + \|f\|_{W^{1,p}(\dot{H}^2)} + \|f\|_{L^p(\dot{H}^{4+\sigma})} + \|f\|_{W^{2,p}(L^2)}) \\
&\quad + Qt^{-\varepsilon} \|\Delta u_0\|_{L^2},
\end{aligned}$$

which completes the proof. \square

4. Second-order scheme. In this section, we propose and analyze a second-order numerical approximation to (1.3)-(1.5).

4.1. Temporal semi-discrete scheme. Denote

$$0 = t_0 < t_1 < \cdots < t_N = T, \quad N \in \mathbb{Z}^+, \quad \tau = t_n - t_{n-1} = \frac{T}{N}, \quad 1 \leq n \leq N.$$

In addition, we define

$$\delta_t V^n = \frac{V^n - V^{n-1}}{\tau}, \quad V^{n-1/2} = \frac{V^n + V^{n-1}}{2}, \quad t_{n-1/2} = \frac{t_n + t_{n-1}}{2}, \quad 1 \leq n \leq N.$$

To facilitate the analysis, we first denote

$$\hat{V}^n = e^{-\lambda t_n} V^n, \quad 1 \leq \lambda < \infty, \quad (4.1)$$

and

$$\delta_t^\lambda \hat{V}^n := \frac{\hat{V}^n - e^{-\lambda \tau} \hat{V}^{n-1}}{\tau} = e^{-\lambda t_n} \delta_t V^n, \quad n \geq 1. \quad (4.2)$$

We employ the linear interpolation quadrature to approximate the integral term in (1.3)

$$\begin{aligned}
I^{(\alpha(t_n))} \varphi(t_n) &= \int_0^{t_n} \frac{(t_n - s)^{\alpha(t_n - s) - 1}}{\Gamma(\alpha(t_n - s))} \varphi(s) ds \\
&\approx \sum_{j=1}^n \int_{t_{j-1}}^{t_j} \frac{(t_n - s)^{\alpha(t_n - s) - 1}}{\Gamma(\alpha(t_n - s))} \mathcal{L}_1[\varphi](s) ds \\
&= \sum_{j=1}^n [a_{n,j} \varphi^j + b_{n,j} \varphi^{j-1}] := II_n(\varphi), \quad n \geq 1,
\end{aligned} \quad (4.3)$$

where

$$\varphi^j = \varphi(t_j), \quad \mathcal{L}_1[\varphi](s) = \frac{s - t_{j-1}}{\tau} \varphi^j + \frac{t_j - s}{\tau} \varphi^{j-1}, \quad (4.4)$$

and

$$\begin{aligned} a_{n,j} &= \int_{t_{j-1}}^{t_j} \frac{(t_n - s)^{\alpha(t_n - s) - 1}}{\Gamma(\alpha(t_n - s))} \frac{s - t_{j-1}}{\tau} ds > 0, \\ b_{n,j} &= \int_{t_{j-1}}^{t_j} \frac{(t_n - s)^{\alpha(t_n - s) - 1}}{\Gamma(\alpha(t_n - s))} \frac{t_j - s}{\tau} ds > 0. \end{aligned} \quad (4.5)$$

Then (1.3) implies

$$\begin{aligned} \frac{1}{2}[I^{(\alpha(t_n))}\varphi(t_n) + I^{(\alpha(t_{n-1}))}\varphi(t_{n-1})] &\approx \frac{1}{2} \sum_{j=1}^n [a_{n,j}\varphi^j + b_{n,j}\varphi^{j-1}] \\ &+ \frac{1}{2} \sum_{j=1}^{n-1} [a_{n-1,j}\varphi^j + b_{n-1,j}\varphi^{j-1}], \quad n \geq 1, \end{aligned} \quad (4.6)$$

and we use the fact that $a_{n-1,j} = a_{n,j+1}$ and $b_{n-1,j} = b_{n,j+1}$ to get

$$\begin{aligned} \frac{1}{2}[I^{(\alpha(t_n))}\varphi(t_n) + I^{(\alpha(t_{n-1}))}\varphi(t_{n-1})] &\approx \sum_{j=1}^n a_{n,j} \frac{\varphi^j + \varphi^{j-1}}{2} \\ &+ \sum_{j=1}^n b_{n,j} \frac{\varphi^{j-1} + \varphi^{j-2}}{2} - a_{n,1} \frac{\varphi^0}{2} := II_{n-1/2}(\varphi), \quad \varphi^{-1} = 0 = II_0(\varphi). \end{aligned} \quad (4.7)$$

Now, we consider (1.3) at the point $t = t_n$ and apply Crank-Nicolson method to get for $u^n := u(\mathbf{x}, t_n)$

$$\delta_t u^n - \mu \Delta u^{n-1/2} - \zeta II_{n-1/2}(\Delta u) = f^{n-1/2} + \mathcal{R}^n, \quad 1 \leq n \leq N, \quad (4.8)$$

$$u^0 = u_0, \quad (4.9)$$

where $\mathcal{R}^n = \mathcal{R}_1^n + \mathcal{R}_2^{n-1/2}$, and

$$\mathcal{R}_1^n = [\delta_t u^n - \partial_t u(t_{n-1/2})] + [\partial_t u(t_{n-1/2}) - (\partial_t u)^{n-1/2}], \quad n \geq 1, \quad (4.10)$$

$$\mathcal{R}_2^n = \zeta(II_n(\Delta u) - I^{(\alpha(t_n))}\Delta u(t_n)), \quad n \geq 1, \quad \mathcal{R}_2^0 = 0. \quad (4.11)$$

By omitting the small term \mathcal{R}^n in (4.8) and replacing U^n as approximate solutions of u^n , we obtain Crank-Nicolson scheme as

$$\delta_t U^n - \mu \Delta U^{n-1/2} - \zeta II_{n-1/2}(\Delta U) = f^{n-1/2}, \quad 1 \leq n \leq N, \quad (4.12)$$

$$U^0 = u_0. \quad (4.13)$$

Then, we use the notation of (4.1) and (4.2) and multiply both sides of (4.12) by $e^{-\lambda t_n}$ to get

$$\begin{aligned} \delta_t^\lambda \hat{U}^n - \mu \Lambda_\lambda(\Delta \hat{U}^n) - \zeta \sum_{j=1}^n \tilde{a}_{n,j} \Lambda_\lambda(\Delta \hat{U}^j) - \zeta \sum_{j=2}^n \tilde{b}_{n,j} \Lambda_\lambda(\Delta \hat{U}^{j-1}) \\ + \zeta(a_{n,1} - b_{n,1})e^{-\lambda t_n} \Lambda_\lambda(\Delta \hat{U}^0) = \Lambda_\lambda(\hat{f}^n), \quad 1 \leq n \leq N, \end{aligned} \quad (4.14)$$

where

$$\tilde{a}_{n,j} = a_{n,j}e^{-\lambda t_{n-j}}, \quad \tilde{b}_{n,j} = b_{n,j}e^{-\lambda t_{n+1-j}}, \quad \Lambda_\lambda(\hat{V}^n) = \frac{\hat{V}^n + e^{-\lambda \tau} \hat{V}^{n-1}}{2}. \quad (4.15)$$

4.2. Stability and error estimate. Next, we shall deduce the following stability result.

THEOREM 4.1. *Let U^m be the solution of the Crank-Nicolson scheme (4.12)-(4.13). Then we have*

$$\|U^m\|^2 \leq Q \left(\|U^0\|^2 + \tau \|\nabla U^0\|^2 + \tau \sum_{n=1}^m \|f^{n-1/2}\|^2 \right), \quad 1 \leq m \leq N.$$

Proof. We first take the inner product of (4.14) with $\tau \Lambda_\lambda(\hat{U}^n)$ and then sum for n from 1 to m to get

$$\begin{aligned} & \tau \sum_{n=1}^m (\delta_t^\lambda \hat{U}^n, \Lambda_\lambda(\hat{U}^n)) + \mu\tau \sum_{n=1}^m (\Lambda_\lambda(\nabla \hat{U}^n), \Lambda_\lambda(\nabla \hat{U}^n)) \\ & + \zeta\tau \sum_{n=1}^m \tilde{a}_{n,n} (\Lambda_\lambda(\nabla \hat{U}^n), \Lambda_\lambda(\nabla \hat{U}^n)) = -\zeta\tau \sum_{n=2}^m \sum_{j=1}^{n-1} \tilde{a}_{n,j} (\Lambda_\lambda(\nabla \hat{U}^j), \Lambda_\lambda(\nabla \hat{U}^n)) \\ & - \zeta\tau \sum_{n=2}^m \sum_{j=2}^n \tilde{b}_{n,j} (\Lambda_\lambda(\nabla \hat{U}^{j-1}), \Lambda_\lambda(\nabla \hat{U}^n)) + \tau \sum_{n=1}^m (\Lambda_\lambda(\hat{f}^n), \Lambda_\lambda(\hat{U}^n)) \\ & + \zeta\tau \sum_{n=1}^m (a_{n,1} - b_{n,1}) e^{-\lambda t_n} (\Lambda_\lambda(\nabla \hat{U}^0), \Lambda_\lambda(\nabla \hat{U}^n)) := -\zeta\Phi_1 - \zeta\Phi_2 + \Phi_4 + \zeta\Phi_3, \end{aligned}$$

which follows from $a_{n,n} \geq 0$ and

$$\begin{aligned} \tau \sum_{n=1}^m (\delta_t^\lambda \hat{U}^n, \Lambda_\lambda(\hat{U}^n)) & = \sum_{n=1}^m \frac{\|\hat{U}^n\|^2 - \|e^{-\lambda\tau} \hat{U}^{n-1}\|^2}{2} \\ & \geq \sum_{n=1}^m \frac{\|\hat{U}^n\|^2 - \|\hat{U}^{n-1}\|^2}{2} = \frac{\|\hat{U}^m\|^2 - \|\hat{U}^0\|^2}{2} \end{aligned} \quad (4.16)$$

that

$$\frac{\|\hat{U}^m\|^2 - \|\hat{U}^0\|^2}{2} + \mu\tau \sum_{n=1}^m \|\Lambda_\lambda(\nabla \hat{U}^n)\|^2 \leq \zeta \sum_{j=1}^3 |\Phi_j| + |\Phi_4|. \quad (4.17)$$

Below we will further estimate the terms of the right-hand side of (4.17). First, we apply Cauchy-Schwarz inequality and $ab \leq \frac{a^2+b^2}{2}$ to obtain

$$\begin{aligned} |\Phi_1| & \leq \tau \sum_{n=2}^m \sum_{j=1}^{n-1} \tilde{a}_{n,j} \|\Lambda_\lambda(\nabla \hat{U}^j)\| \|\Lambda_\lambda(\nabla \hat{U}^n)\| \\ & \leq \tau \sum_{n=2}^m \sum_{j=1}^{n-1} \tilde{a}_{n,j} \frac{\|\Lambda_\lambda(\nabla \hat{U}^j)\|^2 + \|\Lambda_\lambda(\nabla \hat{U}^n)\|^2}{2} \\ & = \tau \sum_{n=2}^m \sum_{j=1}^{n-1} \tilde{a}_{n,j} \frac{\|\Lambda_\lambda(\nabla \hat{U}^j)\|^2}{2} + \tau \sum_{n=2}^m \frac{\|\Lambda_\lambda(\nabla \hat{U}^n)\|^2}{2} \sum_{j=1}^{n-1} \tilde{a}_{n,j} \\ & = \tau \sum_{j=1}^{m-1} \frac{\|\Lambda_\lambda(\nabla \hat{U}^j)\|^2}{2} \sum_{n=j+1}^m \tilde{a}_{n,j} + \tau \sum_{n=2}^m \frac{\|\Lambda_\lambda(\nabla \hat{U}^n)\|^2}{2} \sum_{j=1}^{n-1} \tilde{a}_{n,j}, \end{aligned}$$

where

$$\begin{aligned} \sum_{n=j+1}^m \tilde{a}_{n,j} &\leq Q \sum_{n=j+1}^m e^{-\lambda t_{n-j}} \tau (t_n - t_j)^{\alpha_* - 1} = Q \tau \sum_{p=1}^{m-j} e^{-\lambda t_p} (t_p)^{\alpha_* - 1} \\ &\leq Q \int_0^{t_{m-j}} e^{-\lambda s} s^{\alpha_* - 1} ds \leq Q \int_0^\infty e^{-\lambda s} s^{\alpha_* - 1} ds \leq Q \lambda^{-\alpha_*}, \\ \sum_{\tilde{j}=1}^{n-1} \tilde{a}_{n,j} &\leq Q \sum_{p=1}^{n-1} e^{-\lambda t_p} \tau (t_p)^{\alpha_* - 1} \leq Q \int_0^\infty e^{-\lambda s} s^{\alpha_* - 1} ds \leq Q \lambda^{-\alpha_*}. \end{aligned}$$

Thus, we get

$$|\Phi_1| \leq (Q \lambda^{-\alpha_*}) \tau \sum_{n=1}^m \|\Lambda_\lambda(\nabla \hat{U}^n)\|^2. \quad (4.18)$$

Then, similar to the analysis of (4.18), we use $\tilde{b}_{n,n} \leq Q \int_{t_{n-1}}^{t_n} (t_n - s)^{\alpha_* - 1} ds \leq Q \tau^{\alpha_*}$ to get

$$\begin{aligned} |\Phi_2| &\leq Q \tau \sum_{n=2}^m \tilde{b}_{n,n} \|\Lambda_\lambda(\nabla \hat{U}^{n-1})\| \|\Lambda_\lambda(\nabla \hat{U}^n)\| \\ &\quad + \tau \sum_{n=2}^m \sum_{j=2}^{n-1} \tilde{b}_{n,j} \|\Lambda_\lambda(\nabla \hat{U}^{j-1})\| \|\Lambda_\lambda(\nabla \hat{U}^n)\| \\ &\leq Q (\tau^{\alpha_*} + \lambda^{-\alpha_*}) \tau \sum_{n=1}^m \|\Lambda_\lambda(\nabla \hat{U}^n)\|^2. \end{aligned} \quad (4.19)$$

Next, we discuss the term $|\Phi_3|$. We utilize

$$|a_{1,1} - b_{1,1}| \leq Q \tau^{\alpha_*}, \quad |a_{n,1} - b_{n,1}| \leq Q \tau t_{n-1}^{\alpha_* - 1} \leq Q \tau^{\alpha_*}, \quad n \geq 2,$$

and Cauchy-Schwarz inequality to get

$$\begin{aligned} |\Phi_3| &\leq (Q \tau^{\alpha_*}) \tau \sum_{n=1}^m \|\Lambda_\lambda(\nabla \hat{U}^n)\|^2 + Q \tau^{\alpha_* + 1} \|\Lambda_\lambda(\nabla \hat{U}^0)\|^2 \\ &\quad + \tau \sum_{n=2}^m Q \tau t_{n-1}^{\alpha_* - 1} e^{-\lambda t_{n-1}} \|\Lambda_\lambda(\nabla \hat{U}^0)\|^2 \\ &\leq (Q \tau^{\alpha_*}) \tau \sum_{n=1}^m \|\Lambda_\lambda(\nabla \hat{U}^n)\|^2 + Q \tau \|\Lambda_\lambda(\nabla \hat{U}^0)\|^2. \end{aligned} \quad (4.20)$$

Finally, we bound $|\Phi_4|$. It is easy to obtain with $\Lambda_\lambda(\hat{V}^n) = e^{-\lambda t_n} V^{n-1/2}$,

$$|\Phi_4| \leq Q \tau \sum_{n=1}^m \|\Lambda_\lambda(\hat{U}^n)\| \|\Lambda_\lambda(\hat{f}^n)\| \leq Q \tau \sum_{n=1}^m \|U^{n-1/2}\| \|f^{n-1/2}\|. \quad (4.21)$$

We put (4.18)–(4.21) into the right-hand side of (4.17):

$$\begin{aligned} \frac{\|\hat{U}^m\|^2}{2} + \mu \tau \sum_{n=1}^m \|\Lambda_\lambda(\nabla \hat{U}^n)\|^2 &\leq Q \zeta (\tau^{\alpha_*} + \lambda^{-\alpha_*}) \tau \sum_{n=1}^m \|\Lambda_\lambda(\nabla \hat{U}^n)\|^2 \\ &\quad + Q \zeta \tau \|\Lambda_\lambda(\nabla \hat{U}^0)\|^2 + Q \tau \sum_{n=1}^m \|U^{n-1/2}\| \|f^{n-1/2}\| + \frac{\|\hat{U}^0\|^2}{2}, \end{aligned}$$

in which, taking suitable large λ and small τ so that $Q\zeta(\tau^{\alpha_*} + \lambda^{-\alpha_*}) \leq \mu$, we get

$$\frac{\|\hat{U}^m\|^2}{2} \leq Q\tau \|\Lambda_\lambda(\nabla \hat{U}^0)\|^2 + \frac{\|\hat{U}^0\|^2}{2} + Q\tau \sum_{n=1}^m \|U^{n-1/2}\| \|f^{n-1/2}\|, \quad (4.22)$$

which combines the estimate

$$Q\tau \sum_{n=1}^m \|U^{n-1/2}\| \|f^{n-1/2}\| \leq Q\tau \|U^m\|^2 + Q\tau \sum_{n=0}^{m-1} \|U^n\|^2 + Q\tau \sum_{n=1}^m \|f^{n-1/2}\|^2,$$

$\frac{\|\hat{U}^m\|^2}{2} = \frac{e^{-2\lambda t_m} \|U^m\|^2}{2}$, and $2Qe^{2\lambda t_m} \tau \leq \frac{1}{4}$ yields

$$\frac{\|U^m\|^2}{4} \leq Q\tau \|\nabla U^0\|^2 + \frac{\|U^0\|^2}{2} + Q\tau \sum_{n=1}^m \|f^{n-1/2}\|^2 + Q\tau \sum_{n=0}^{m-1} \|U^n\|^2.$$

This finishes the proof by the discrete Grönwall's inequality. \square

In what follows, we shall deduce the convergence of the Crank-Nicolson scheme (4.12)-(4.13). By subtracting (4.12)-(4.13) from (4.8)-(4.9), we arrive at the following error equations

$$\delta_t \rho^n - \mu \Delta \rho^{n-1/2} - \zeta II_{n-1/2}(\Delta \rho) = \mathcal{R}^n, \quad 1 \leq n \leq N, \quad (4.23)$$

$$\rho^0 = 0. \quad (4.24)$$

Then, we use (4.14) to get for $1 \leq n \leq N$

$$\delta_t^\lambda \hat{\rho}^n - \mu \Lambda_\lambda(\Delta \hat{\rho}^n) - \zeta \sum_{j=1}^n \tilde{a}_{n,j} \Lambda_\lambda(\Delta \hat{\rho}^j) - \zeta \sum_{j=2}^n \tilde{b}_{n,j} \Lambda_\lambda(\Delta \hat{\rho}^{j-1}) = \hat{\mathcal{R}}^n. \quad (4.25)$$

THEOREM 4.2. *Under the conditions of Theorem 3.5, the following error estimate holds with $T < \infty$*

$$\|u^m - U^m\| \leq Q\tau^2, \quad 1 \leq m \leq N.$$

Proof. Based on the analysis of Theorem 4.1 and (4.22), we use (4.25) to get

$$\frac{\|\hat{\rho}^m\|^2}{2} \leq Q\tau \sum_{n=1}^m \|\rho^{n-1/2}\| \|\hat{\mathcal{R}}^n\| \leq Q\tau \sum_{n=1}^m \|\rho^{n-1/2}\| \|\mathcal{R}^n\|,$$

which further gives

$$\|\rho^m\|^2 \leq Q\tau \sum_{n=1}^m \|\rho^{n-1/2}\| \|\mathcal{R}^n\|.$$

Then, selecting a suitable m_* such that $\|\rho^{m_*}\| = \max_{0 \leq n \leq m} \|\rho^n\|$, we have

$$\|\rho^m\| \leq \|\rho^{m_*}\| \leq Q\tau \sum_{n=1}^{m_*} \|\mathcal{R}^n\| \leq Q\tau \sum_{n=1}^m \left(\|\mathcal{R}_1^n\| + \|\mathcal{R}_2^{n-1/2}\| \right). \quad (4.26)$$

Next, we will discuss the terms of the right-hand side of (4.26). By Taylor expansion with integral remainder, (4.10) gives

$$\|\mathcal{R}_1^1\| \leq 2 \int_0^\tau \|\partial_t^2 u(t)\| dt, \quad \|\mathcal{R}_1^n\| \leq \tau \int_{t_{n-1}}^{t_n} \|\partial_t^3 u(t)\| dt, \quad n \geq 2,$$

which combines (3.4) and (3.6), then we get

$$\tau \sum_{n=1}^m \|\mathcal{R}_1^n\| \leq Q\tau^2 + Q\tau^2 \int_{t_1}^{t_m} t^{-\varepsilon} dt \leq Q\tau^2. \quad (4.27)$$

We apply the remainder of linear interpolation with $\xi_j \in (t_{j-1}, t_j)$, (4.11), (4.4), and (3.5) to get

$$\begin{aligned} \|\mathcal{R}_2^n\| &\leq \zeta \sum_{j=1}^n \int_{t_{j-1}}^{t_j} \frac{(t_n - s)^{\alpha(t_n - s) - 1}}{\Gamma(\alpha(t_n - s))} \|\Delta u(s) - \mathcal{L}_1[\Delta u](s)\| ds \\ &\leq Q \sum_{j=1}^n \int_{t_{j-1}}^{t_j} (t_n - s)^{\alpha_* - 1} \left\| \frac{1}{2} \partial_t^2 \Delta u(\xi_j)(s - t_j)(s - t_{j-1}) \right\| ds \\ &\leq Q \sum_{j=1}^n \int_{t_{j-1}}^{t_j} (t_n - s)^{\alpha_* - 1} \|\partial_t^2 \Delta u(\xi_j)\| \frac{\tau^2}{2} ds \\ &\leq Q\tau^2 \int_0^{t_n} (t_n - s)^{\alpha_* - 1} ds. \end{aligned}$$

Thus we further obtain

$$\tau \sum_{n=1}^m \|\mathcal{R}_2^n\| \leq Q\tau^3 \sum_{n=1}^m \int_0^{t_n} (t_n - s)^{\alpha_* - 1} ds \leq Q\tau^2. \quad (4.28)$$

By inserting (4.27) and (4.28) into (4.26), the proof is completed. \square

4.3. Fully discrete scheme. Next, we shall develop a fully discrete Crank-Nicolson scheme by applying the spatial finite element method. Define a quasi-uniform partition of Ω with the mesh diameter h . Let S_h be the space of continuous piecewise linear functions on Ω with respect to the partition. Define the Ritz projector $I_h : H_0^1(\Omega) \rightarrow S_h$ by

$$(\nabla(I_h w - w), \nabla \chi) = 0 \quad \text{for } \chi \in S_h$$

with the following approximation property [19]

$$\|w - I_h w\|_{L^2} \leq Qh^2 \|w(t)\|_{H^2(\Omega)}. \quad (4.29)$$

Based on the Crank-Nicolson scheme (4.12)-(4.13), we obtain the fully discrete Galerkin scheme: find $\hat{U}_h \in S_h$ such that

$$\begin{aligned} & \left(\delta_t^\lambda \hat{U}_h^n, \chi \right) + \mu \left(\Lambda_\lambda(\nabla \hat{U}_h^n), \nabla \chi \right) \\ & + \zeta \sum_{j=1}^n \tilde{a}_{n,j} \left(\Lambda_\lambda(\nabla \hat{U}_h^j), \nabla \chi \right) + \zeta \sum_{j=2}^n \tilde{b}_{n,j} \left(\Lambda_\lambda(\nabla \hat{U}_h^{j-1}), \nabla \chi \right) \\ & - \zeta(a_{n,1} - b_{n,1}) e^{-\lambda t_n} \left(\Lambda_\lambda(\nabla \hat{U}_h^0), \nabla \chi \right) = \left(\Lambda_\lambda(\hat{f}^n), \chi \right), \quad 1 \leq n \leq N, \end{aligned} \quad (4.30)$$

for all $\chi \in S_h$ with the suitable approximation $U_h^0 \approx u_0$.

To facilitate analysis, we decompose

$$u(t_n) - U_h^n = \zeta^n - \eta(t_n) := \zeta^n - \eta^n,$$

where

$$\zeta^n = I_h u(t_n) - U_h^n \in S_h, \quad \eta^n = I_h u(t_n) - u(t_n). \quad (4.31)$$

We apply (4.8), (4.31), and (4.30) to get the following error equation

$$\begin{aligned} & \left(\delta_t^\lambda \hat{\zeta}^n, \chi \right) + \mu \left(\Lambda_\lambda(\nabla \hat{\zeta}^n), \nabla \chi \right) + \zeta \sum_{j=1}^n \tilde{a}_{n,j} \left(\Lambda_\lambda(\nabla \hat{\zeta}^j), \nabla \chi \right) \\ & + \zeta \sum_{j=2}^n \tilde{b}_{n,j} \left(\Lambda_\lambda(\nabla \hat{\zeta}^{j-1}), \nabla \chi \right) = \left(\hat{\mathcal{R}}^n + \delta_t^\lambda \hat{\eta}^n, \chi \right), \quad 1 \leq n \leq N. \end{aligned} \quad (4.32)$$

THEOREM 4.3. *Let U_h^m be the solution of the fully discrete Crank-Nicolson Galerkin scheme (4.30). Then the following stability result holds*

$$\|U_h^m\|^2 \leq Q \left(\|U_h^0\|^2 + \tau \|\nabla U_h^0\|^2 + \tau \sum_{n=1}^m \|f^{n-1/2}\|^2 \right), \quad 1 \leq m \leq N. \quad (4.33)$$

In addition, under the conditions of Theorem 3.5, the following error estimate holds

$$\|u^m - U_h^m\| \leq Q(\tau^2 + h^2), \quad 1 \leq m \leq N. \quad (4.34)$$

Proof. We take $\chi = \Lambda_\lambda(\hat{U}_h^n)$ in (4.30) and follow the similar procedures in Theorem 4.1 to obtain (4.33). We then take $\chi = \Lambda_\lambda(\hat{\zeta}^n)$ in (4.32), use $\|\hat{\eta}^m\| \leq Qh^2\|u\|_{L^\infty(H^2)}$, and combine Theorem 4.2 to prove (4.34). \square

5. Numerical simulation. We carry out numerical experiments to investigate the convergence behavior of different discretization schemes (i.e. the second-order scheme (4.30) and the first-order scheme in [40]) and to substantiate the theoretical findings proved in §4. We then numerically investigate the behavior of solutions to model (1.3)-(1.5) to show its dependence on the parameters. Finally, we show the crossover dynamics of (1.3)-(1.5) in mechanical vibration to demonstrate the advantage of introducing variable exponent.

5.1. Convergence test. We consider the problem (1.3)-(1.5) with $\Omega = (0, 1)$, $\mu = \zeta = 1$, $T = 1$, $\alpha(t) = 1 - \frac{4}{5}t$, $u_0(x) = \sin(\pi x)$ and $f = 1$. We fix $M = 32$ (M is the degree of freedom in spatial discretization) to test the temporal convergence rates of the fully discrete second-order scheme (4.30) and the first-order scheme proposed in [40], while we fix $N = 32$ to test its spatial convergence rates. We denote the temporal errors and the convergence rate as

$$E_2(\tau, h) = \sqrt{h \sum_{j=1}^{J-1} |U_j^N(\tau, h) - U_j^{2N}(\tau/2, h)|^2}, \quad \text{rate}^t = \log_2 \left(\frac{E_2(2\tau, h)}{E_2(\tau, h)} \right),$$

and the spatial errors and the corresponding convergence orders are denoted as follows

$$F_2(\tau, h) = \sqrt{h \sum_{j=1}^{J-1} |U_j^N(\tau, h) - U_{2j}^N(\tau, h/2)|^2}, \quad \text{rate}^x = \log_2 \left(\frac{F_2(\tau, 2h)}{F_2(\tau, h)} \right).$$

Numerical results are presented in Table 5.1, which indicate the second-order accuracy of the scheme (4.30) in both space and time that is consistent with Theorem 4.3. Furthermore, the numerical errors of the second-order scheme (4.30) in Table 5.1 are much smaller than those of the first-order scheme proposed in [40], which demonstrates its advantages.

Table 5.1: Discrete L^2 errors and convergence rates of the schemes.

M	Scheme (4.30)		N	Scheme (4.30)		N	Scheme in [40]	
	$E_2(\Delta t, h)$	rate ^x		$E_2(\Delta t, h)$	rate ^t		$E_2(\Delta t, h)$	rate ^t
32	3.5833×10^{-5}	*	64	7.1473×10^{-6}	*	64	2.6569×10^{-4}	*
64	9.0121×10^{-6}	1.99	128	1.7857×10^{-6}	2.00	128	1.3529×10^{-4}	0.97
128	2.2589×10^{-6}	2.00	256	4.4796×10^{-7}	2.00	256	6.8202×10^{-5}	0.99
256	5.6559×10^{-7}	2.00	512	1.1239×10^{-7}	1.99	512	3.4232×10^{-5}	0.99
512	1.4153×10^{-7}	2.00	1024	2.8200×10^{-8}	1.99	1024	1.7147×10^{-5}	1.00
Theory		2.00			2.00			1.00

5.2. Solutions under different parameters. We investigate the solutions to problem (1.3)-(1.5) and its dependence on the parameters. Let $\Omega = (0, 1)$, $[0, T] = [0, 10]$, $u_0 = 0$, $\mu = 0.1$, $\zeta = 1$, and $f = e^{-(t + \frac{(x-0.5)^2}{2})}$, which is roughly an initial point source located at the center $x = 0.5$ of Ω . To test the effects of the exponent, we select $\alpha(t) \equiv \alpha$ for different $0 < \alpha < 1$ and compute $u(0.5, t)$ with $M = 128$ and $N = 1024$ in Fig. 5.1(left), which indicates that: (i) For the case $\alpha = 1$, the solution exhibits the wave propagation behavior with decreasing amplitude over time [6, 7], which corresponds to the fact that the kernel k becomes the identity such that the governing equation (1.3) could be reformulated as a wave equation with a damping term; (ii) For the case $\alpha < 1$, the wave behavior is weakened due to the viscoelastic property of the governing equation.

To investigate the effects of the viscosity μ , we present the solution curves in Fig. 5.2(right) under the same data and $\alpha(t) = 1 - \frac{t}{20}$, from which we observe that the maximum amplitudes of the solutions decrease as μ increases, which reveals the greater dissipation effects under the larger viscosity μ .

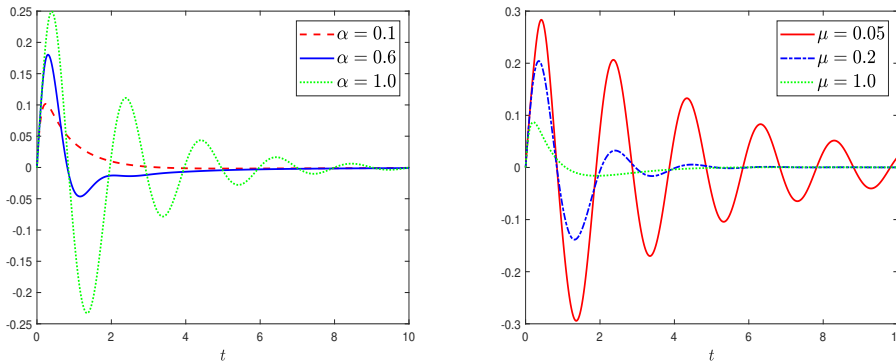


Fig. 5.1: Solution curves of $u(0.5, t)$ under different parameters.

5.3. Crossover dynamics in mechanical vibration. We show the crossover dynamics of model (1.3)-(1.5) in mechanical vibration. Let $\Omega = (0, 10)$, $[0, T] = [0, 150]$, $\mu = 0.4$, $\zeta = 0.05$, $u_0 = 0$, $f = e^{-[\frac{t}{2} + \frac{(x-5)^2}{8}]}$, $M = 128$ and $N = 512$. We plot the solution curves of $u(5, t)$ under different kernels in (1.2) in Fig. 5.2, from which we observe that the solution under the multiscale kernel k coincides with that under the quasi-exponential kernel k_0 within a relatively short temporal interval, and then gradually captures the long-term viscoelastic behavior modeled by the equation (1.3) with the power-law kernel k_∞ . Such transition indicates the capability of the multiscale kernel k in modeling the crossover dynamics due to, e.g. the change of material properties caused by fatigue and deformation.

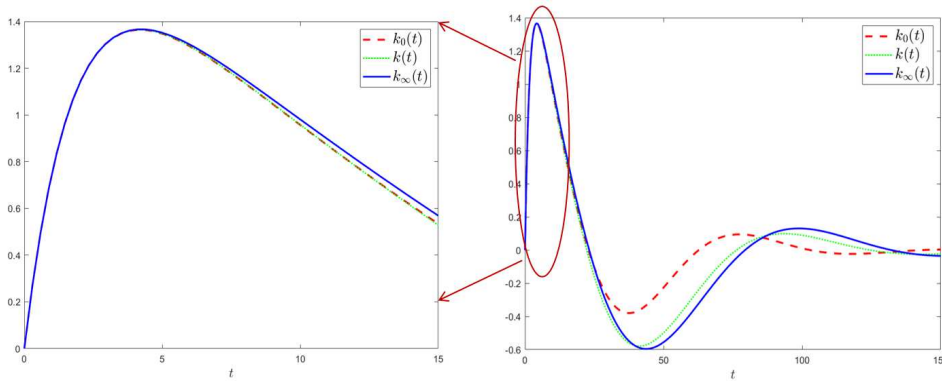


Fig. 5.2: Solution curves of $u(5, t)$ under different kernels.

Acknowledgments. This work was partially supported by the National Natural Science Foundation of China (12301555, 12271303), the National Key R&D Program of China (2023YFA1008903), the Taishan Scholars Program of Shandong Province (tsqn202306083), the Natural Science Foundation of Shandong Province for Outstanding Youth Scholars (ZR2024JQ008), the Major Fundamental Research Project of Shandong Province of China (ZR2023ZD33), and the Postdoctoral Fellowship Program of CPSF (GZC20240938).

REFERENCES

- [1] R. Adams and J. Fournier, Sobolev Spaces, Elsevier, San Diego, 2003.
- [2] G. Akrivis, B. Li, and C. Lubich, *Combining maximal regularity and energy estimates for time discretizations of quasilinear parabolic equations*, Math. Comp., 86 (2017), 1527–1552.
- [3] A. Bonfanti, J. L. Kaplan, G. Charras, A. Kabl, *Fractional viscoelastic models for power-law materials*, Soft Matter, 16 (2020), 6002–6020.
- [4] J. R. Cannon, Y. Lin, *A priori L^2 error estimates for finite-element methods for nonlinear diffusion equations with memory*, SIAM J. Numer. Anal., 27 (1990), 595–607.
- [5] C. Chen, V. Thomée, L. B. Wahlbin, *Finite element approximation of a parabolic integro-differential equation with a weakly singular kernel*, Math. Comp., 58 (1992), 587–602.
- [6] S. W. Cheung, E. T. Chung, Y. Efendiev, W. T. Leung, *Explicit and energy-conserving constraint energy minimizing generalized multiscale discontinuous Galerkin method for wave propagation in heterogeneous media*, Multiscale Model. Simul., 19 (2021), 1736–1759.
- [7] E. T. Chung, Y. Efendiev, R. L. Gibson, M. Vasilyeva, *A generalized multiscale finite element method for elastic wave propagation in fractured media*, GEM-Int. J. Geomath., 7 (2016), 163–182.

- [8] R. Dang, Y. Cui, J. Qu, A. Yang, Y. Chen, *Variable fractional modeling and vibration analysis of variable-thickness viscoelastic circular plate*, Appl. Math. Model., 110 (2022), 767–778.
- [9] W. Deng, B. Li, W. Tian, and P. Zhang, *Boundary problems for the fractional and tempered fractional operators*, Multiscale Model. Simul., 16 (2018), 125–149.
- [10] H. Engler, *On the dynamic shear flow problem for viscoelastic liquids*, SIAM J. Math. Anal., 18 (1987), 972–990.
- [11] L. Evans, *Partial Differential Equations*, Graduate Studies in Mathematics, Graduate Studies in Mathematics, V 19, American Mathematical Society, Rhode Island, 1998.
- [12] W. Fan, X. Hu, and S. Zhu, *Numerical reconstruction of a discontinuous diffusive coefficient in variable-order time-fractional subdiffusion*, J. Sci. Comput., 96 (2023), 13.
- [13] A. Friedman, M. Shinbrot, *Volterra integral equations in Banach space*, Trans. Amer. Math. Soc., 126 (1967), 31–179.
- [14] Z. Hao, W. Cao, G. Lin, *A second-order difference scheme for the time fractional substantial diffusion equation*, J. Comput. Appl. Math., 313 (2017), 54–69.
- [15] M. L. Heard, *An abstract parabolic Volterra integrodifferential equation*, SIAM J. Math. Anal., 13 (1982), 81–105.
- [16] M. L. Heard, S. M. Rankin III, *A semilinear parabolic Volterra integrodifferential equation*, J. Differential Equ., 71 (1988), 201–233.
- [17] J. Jeon, N. Leijnse, L. Oddershede, R. Metzler, *Anomalous diffusion and power-law relaxation of the time averaged mean squared displacement in worm-like micellar solutions*, New J. Phys., 15 (2013), 045011.
- [18] L. Jiang and N. Ou, *Bayesian inference using intermediate distribution based on coarse multiscale model for time fractional diffusion equations*, Multiscale Model. Simul., 16 (2018), 327–355.
- [19] B. Jin, *Fractional differential equations—an approach via fractional derivatives*, Appl. Math. Sci. 206, Springer, Cham, 2021.
- [20] S. Larsson, V. Thomée, L. Wahlbin, *Numerical solution of parabolic integro-differential equations by the discontinuous Galerkin method*, Math. Comp., 67 (1998), 45–71.
- [21] Y. Li, H. Wang, and X. Zheng, *Analysis of a fractional viscoelastic Euler-Bernoulli beam and identification of its piecewise continuous polynomial order*, Fract. Calc. Appl. Anal., 26 (2023), 2337–2360.
- [22] C. Lorenzo and T. Hartley, *Variable order and distributed order fractional operators*, Nonlinear Dyn., 29 (2002), 57–98.
- [23] C. Lubich, *Convolution quadrature and discretized operational calculus. I and II.*, Numer. Math., 52 (1988), 129–145 and 413–425.
- [24] W. McLean, I. H. Sloan, V. Thomée, *Time discretization via Laplace transformation of an integro-differential equation of parabolic type*, Numer. Math., 102 (2006), 497–522.
- [25] M. Meerschaert, A. Sikorskii, *Stochastic Models for Fractional Calculus*, De Gruyter Studies in Mathematics, 2011.
- [26] R. Meng, D. Yin, and C. Drapaca, *Variable-order fractional description of compression deformation of amorphous glassy polymers*, Comput. Mech., 64 (2019), 163–171.
- [27] S. Mukherjee, P. Pareek, M. Barma, and S. Nandi, *Stretched exponential to power-law: crossover of relaxation in a kinetically constrained model*, J. Stat. Mech.: Theory Exp., 2024 (2024), 023205.
- [28] K. Mustapha, H. Mustapha, *A second-order accurate numerical method for a semilinear integro-differential equation with a weakly singular kernel*, IMA J. Numer. Anal., 30 (2010), 555–578.
- [29] K. Mustapha, H. Brunner, H. Mustapha, D. Schötzau, *An hp-version discontinuous Galerkin method for integro-differential equations of parabolic type*, SIAM J. Numer. Anal., 49 (2011), 1369–1396.
- [30] J. Orosco, C. F. M. Coimbra, *Variable-order modeling of nonlocal emergence in many-body systems: Application to radiative dispersion*, Phys. Rev. E, 98 (2018), 032208.
- [31] A. K. Pani, G. Fairweather, R. I. Fernandes, *ADI orthogonal spline collocation methods for parabolic partial integro-differential equations*, IMA J. Numer. Anal., 30 (2010), 248–276.
- [32] I. Podlubny, *Fractional Differential Equations*, Academic Press, 1999.
- [33] L. Qiao, D. Xu, *Compact alternating direction implicit scheme for integro-differential equations of parabolic type*, J. Sci. Comput., 76 (2018), 565–582.
- [34] W. Qiu, *Optimal error estimate of an accurate second-order scheme for Volterra integrodifferential equations with tempered multi-term kernels*, Adv. Comput. Math., 49 (2023), 43.
- [35] H. Sun, A. Chang, Y. Zhang, and W. Chen, *A review on variable-order fractional differential equations: Mathematical foundations, physical models, numerical methods and applica-*

- tions, *Fract. Calc. Appl. Anal.*, 22 (2019), 27–59.
- [36] D. Xu, *Uniform l^1 Behavior for Time Discretization of a Volterra Equation with Completely Monotonic Kernel II: Convergence*, *SIAM J. Numer. Anal.*, 46 (2008), 231–259.
- [37] D. Xu, *Stability of the difference type methods for linear Volterra equations in Hilbert spaces*, *Numer. Math.*, 109 (2008), 571–595.
- [38] Y. Yan, G. Fairweather, *Orthogonal spline collocation methods for some partial integrodifferential equations*, *SIAM J. Numer. Anal.*, 29 (1992), 755–768.
- [39] H. M. Yin, *On parabolic Volterra equations in several space dimensions*, *SIAM J. Math. Anal.*, 22 (1991), 1723–1737.
- [40] X. Zheng, Y. Li, W. Qiu, *Local modification of subdiffusion by initial Fickian diffusion: Multiscale modeling, analysis, and computation*, *Multiscale Model. Simul.*, 22 (2024), 1534–1557.